Structure, Bonding, and Dipole Moment of $(CH_3)_3N-SO_3$. A Microwave Study

D. L. Fiacco, A. Toro,† and K. R. Leopold*

Department of Chemistry, University of Minnesota, 207 Pleasant St. SE, Minneapolis, Minnesota 55455

Received August 3, 1999

Six isotopic derivatives of the complex $(CH_3)_3N-SO_3$ have been studied in the gas phase by microwave spectroscopy. The N−S bond length is 1.912(20) Å, and the NSO angle is 100.1(2)°. The dipole moment, determined from Stark effect measurements, is 7.1110(69) D, representing an enhancement of 6.5 D over the sum of the dipole moments of the free monomers. Analysis of the ^{14}N nuclear hyperfine structure indicates that about 0.6 e is transferred from the nitrogen to the SO_3 upon formation of the complex. Comparison between the gas-phase structure and that previously determined for the adduct in the solid state reveals small but significant differences, indicating that the formation of the dative bond is slightly less advanced in the gas. Gas-phase and solid-state structural data are compared for several related amine−SO_3 systems.

Introduction

Recently in our laboratory we have been concerned with the structure and bonding of electron pair donor−acceptor complexes, primarily involving BF_3 and SO_3.[1,2] Using microwave spectroscopy,[3−9] and in some cases X-ray diffraction,[10,11] we have investigated a series of adducts of these acids with nitrogen,[3−6,10] oxygen,[7] and halogen[8,9] donors. We have found that, by suitable choice of the acid−base pair, the nature of the dative bond in the gas phase can be adjusted in a near-continuous manner between that of a van der Waals interaction and that of a fully developed chemical bond. Moreover, we observe that adducts whose dative linkage lies in the intermediate regime between bonded and nonbonded interactions display extraordinary changes in structure upon crystallization. Indeed, bond length differences as much as 0.84 Å have been observed between the gas phase and the solid state.[10]

Among the systems we have investigated is the gas-phase zwitterion of sulfamic acid ($^+H_3N-SO_3^-$).[5] Prior to our work, the solid-state structure of this compound had been well characterized by X-ray and neutron diffraction techniques,[12−14] but several *ab initio* studies had been unable to reproduce the observed solid-state structure.[15,16] In 1992, Wong, Wiberg, and Frisch[17] applied the self-consistent reaction field (SCRF) model and showed the zwitterion undergoes significant changes in structure and bonding when placed in a dielectric continuum. The implication was that the disparity between the experimental and theoretical results did not arise from computational deficiency but rather resulted from the real influence of the crystalline environment on the nature of the zwitterion. The structure determined from microwave spectroscopy[5a] turned out to be in excellent agreement with the computational results and demonstrated that the N−S bond length indeed contracts by 0.186(23) Å upon crystallization.

The complex $(CH_3)_3N-SO_3$ is another classic example of a Lewis acid−base adduct, and its comparison with the analogous complex of ammonia should be of fundamental interest with regard to the nature of the dative bond in the gas phase. Several previous studies of this system have been reported, including X-ray diffraction,[18] matrix isolation,[19] and solution-phase kinetic and thermochemical[20,21] measurements. However, the microwave spectrum and gas-phase structure have not been investigated. In this paper, therefore, we present a microwave study of $(CH_3)_3N-SO_3$ in the gas phase. In addition to elucidating the molecular structure, aspects of electronic structure are also determined from measurement of the molecular dipole moment and ^{14}N nuclear hyperfine interactions. The results are compared with those previously reported for H_3N-SO_3, and the observed gas-to-solid structure changes for both compounds are discussed in the context of their known crystal structures.

* To whom correspondence should be addressed.
† Present address: Department of Chemistry, Rutgers, The State University of New Jersey, 610 Taylor Rd, Piscataway, NJ 08855-0939.

(1) Leopold, K. R. In *Advances in Molecular Structure Research*; Hargittai, M., Hargittai, I., Eds.; JAI Press: Greenwich, CT, 1996; Vol. 2, p 103.
(2) Leopold, K. R.; Canagaratna, M.; Phillips, J. A. *Acc. Chem. Res.* **1997**, *30*, 57.
(3) Dvorak, M. A.; Ford, R. S.; Suenram, R. D.; Lovas, F. J.; Leopold, K. R. *J. Am. Chem. Soc.* **1992**, *114*, 108.
(4) Reeve, S. W.; Burns, W. A.; Lovas, F. J.; Suenram, R. D.; Leopold, K. R. *J. Phys. Chem.* **1993**, *97*, 10630.
(5) (a) Canagaratna, M.; Phillips, J. A.; Goodfriend, H.; Leopold, K. R. *J. Am. Chem. Soc.* **1996**, *118*, 5290. (b) Canagaratna, M.; Ott, M. E.; Leopold, K. R. *Chem. Phys. Lett.* **1997**, *281*, 63.
(6) Burns, W. A.; Phillips, J. A.; Canagaratna, M.; Goodfriend, H.; Leopold, K. R. *J. Phys. Chem.* **1999**, *103*, 7445.
(7) Phillips, J. A.; Canagaratna, M.; Goodfriend, H.; Leopold, K. R. *J. Phys. Chem.* **1995**, *99*, 501.
(8) Phillips, J. A.; Canagaratna, M.; Goodfriend, H.; Grushow, A.; Almlöf, J.; Leopold, K. R. *J. Am. Chem. Soc.* **1995**, *117*, 12549.
(9) Canagaratna, M.; Phillips, J. A.; Goodfriend, H.; Fiacco, D. L.; Ott, M. E.; Harms, B.; Leopold, K. R. *J. Mol. Spectrosc.* **1998**, *192*, 338.
(10) Burns, W. A.; Leopold, K. R. *J. Am. Chem. Soc.* **1993**, *115*, 11622.
(11) Phillips, J. A.; Britton, D.; Leopold, K. R. *J. Chem. Crystallogr.* **1996**, *26*, 533.
(12) Kanda, F. A.; King, A. J. *J. Am. Chem. Soc*, **1951**, *73*, 2315.
(13) Sass, R. L. *Acta Crystallogr.* **1960**, *13*, 320.
(14) Bats, J. W.; Coppens, P.; Koetzle, T. F. *Acta Crystallogr.* **1977**, *B33*, 37.
(15) Douglas, J. E.; Kenyon, G. L.; Kollman, P. A. *Chem. Phys. Lett.* **1978**, *57*, 553.
(16) Hickling, S. J.; Woolley, R. G. *Chem. Phys. Lett.* **1990**, *166*, 43.
(17) Wong, M. W.; Wiberg, K. B.; Frisch, M. J. *J. Am. Chem. Soc.* **1992**, *114*, 523.
(18) Morris, A. J.; Kennard, C. H. L.; Hall, J. R.; Smith, G.; White, A. H. *Acta Crystallogr.* **1983**, *C39*, 81.
(19) Sass, C. S.; Ault, B. S. *J. Phys. Chem.* **1986**, *90*, 1547.
(20) Krueger, J. H.; Johnson, W. A. *Inorg. Chem.* **1968**, *7*, 679.
(21) Blandamer, M. J.; Burgess, J.; Duce, P. P. *J. Inorg. Nucl. Chem.* **1981**, *43*, 3103.

10.1021/ic990925j CCC: $19.00
Published on Web 12/11/1999

Experimental Section

Rotational spectra of six isotopomers of $(CH_3)_3N-SO_3$ were obtained using a Balle−Flygare-type pulsed-nozzle Fourier transform microwave spectrometer,[22] the details of which have been described elsewhere.[8,23] Briefly, it consists of a cylindrical Fabry−Perot cavity composed of two circular aluminum mirrors (84 cm radius of curvature) housed in a chamber evacuated with a 20 in. diffusion pump. Molecules produced in a supersonic expansion enter the cavity traveling perpendicular to its axis, and a 1.5−1.7 μs radiation pulse creates a coherent excitation of the molecular sample. The subsequent free induction decay is heterodyne detected and the resulting signal digitized and Fourier transformed to produce a frequency domain spectrum. The range of the instrument is 3−18 GHz, with a resolution of approximately 3 kHz.

Since trimethylamine (TMA) and SO_3 react in the bulk to form solid TMA-SO_3, a co-injection source similar to that employed elsewhere[24−27] was utilized in this study. Argon at a backing pressure of approximately 2 atm was flowed over a solid sample of polymerized SO_3 maintained at 0 °C. The resulting Ar/SO_3 mixture was pulsed at a rate of 6 Hz through a 0.8 mm diameter nozzle orifice. Pure TMA at a pressure of approximately 0.06 atm was continuously injected into the expansion through a 0.012 in. i.d. stainless steel needle. The needle was inserted into the expansion 0.2 in. below the nozzle orifice and was bent at a 90° angle to achieve directed flow along the expansion axis. Nine free induction decays of the molecular polarization, each containing 256 data points, were collected per gas pulse, and the time domain signals were averaged over a minimum of 270 gas pulses. An airlock, which is employed on our system for facile removal of the nozzle from the vacuum chamber, was particularly important in the present study due to frequent clogging of the needle by solid TMA-SO_3.

For the determination of the molecular dipole moment, a pair of parallel 30 × 40 cm aluminum plates straddle the cavity to provide a uniform electric field which is perpendicular to both the cavity axis and the supersonic expansion. Equal and opposite dc voltages were applied to each plate to reduce the effect of fringing fields. The distance between the plates was calibrated as previously described[5b] by measuring the first-order Stark shift on the $J = 4 \leftarrow 3$, $K = \pm 3$ transition of Ar−SO_3, for which the dipole moment has been previously determined (0.2676 ± 0.0003 D).[28] Although this procedure employs a secondary standard in favor of the more conventional OCS primary standard, the first-order Stark effect permits the measurement of larger Stark shifts and hence a slightly more accurate value for the interplate spacing. To eliminate possible effects due to the accumulation of diffusion pump oil on the plate surfaces,[5b,29] calibrated plate distances were obtained both before and after the collection of experimental data. Data were admitted for analysis only upon agreement of the pre- and postcollection values.

Initial spectral searches were guided by an estimation of the rotational constant of TMA-SO_3 obtained from the known gas-phase structures of both TMA and SO_3 monomers[30,31] and estimates of the N−S bond length in the complex. The spectral peaks due to the TMA−SO_3 complex were identified by their dependence on both TMA and SO_3 as well as the characteristic hyperfine splittings due to the ^{14}N nucleus. Further confirmation of their identity was obtained by the close agreement between the observed and predicted rotational spectra for the ^{15}N- and ^{34}S-containing species. The ^{15}N/^{32}S and ^{14}N/^{33}S isotopomers were observed in natural abundance. For the ^{15}N/^{34}S and ^{15}N/^{33}S derivatives, [^{15}N]trimethylamine was synthesized according to literature procedures:[32] $(CH_3)_3H^{15}N^+Cl^-$ was prepared from the reaction of $^{15}NH_4Cl$ (99.5 atom %, Icon Services) and paraformaldehyde (Aldrich) and the free amine released by reaction with NaOH.

Results

The observed frequencies for the $J = 1 \leftarrow 0$, $2 \leftarrow 1$, $3 \leftarrow 2$, and $4 \leftarrow 3$ transitions of the parent isotopomer are listed in Table 1. Tables 2−4 list the observed frequencies for the ^{34}S-, ^{33}S-, and ^{15}N-containing species. The spectra were characteristic of a semirigid symmetric rotor with no evidence of internal rotation. A representative spectrum is shown in Figure 1.

Analysis of the spectra was carried out using standard methods. The frequencies for each isotopomer were fit to the usual expression[33] for a symmetric top with one or two quadrupolar nuclei, as appropriate, viz.

$$\nu = 2(J'' + 1)[B - D_{JK}K^2] - 4D_J(J'' + 1)^3 + \Delta E_Q \quad (1)$$

Here, ΔE_Q is the difference in hyperfine energies between the upper and lower states and was adequately calculated via the usual first-order treatment for the ^{14}N- and ^{33}S-containing species. The other symbols have their usual meanings.[33] Least-squares fits of the observed spectral frequencies were carried out for each of the isotopomers investigated, and the fitted spectroscopic constants are given in Table 5. The value of D_{JK} in eq 1 was found to be vanishingly small and was constrained to zero in the final fits.

Three sets of Stark shifted transitions were investigated, corresponding to the $J = 1 \leftarrow 0$ and $2 \leftarrow 1$, $K = 0, \pm 1$ of the parent species. A detailed list containing 74 observed Stark-hyperfine components at electric field strengths from 0.42 to 37.01 V/cm is available as Supporting Information. Both parallel ($\Delta M_F = 0$) and perpendicular ($\Delta M_F = \pm 1$) components were observed, corresponding to either a parallel or perpendicular orientation of the oscillating microwave field with respect to the applied electric field. The low intensity as well as the large first-order Stark shifts of the $K = \pm 1$ components limited the applicable field strengths to less than 10 V/cm. Greater field strengths were utilized in the examination of the $K = 0$ components, which are susceptible only to a much weaker second-order Stark effect, and hence smaller Stark shifts. A sample spectrum, taken at 18.59 V/cm, is shown in Figure 2.

The Stark-hyperfine energies were calculated in the intermediate field regime using a $|J, K, I, M_I, M_J, M_F\rangle$ basis as previously described.[5b,33] A nonlinear least-squares fit of the

(22) (a) Balle, T. J.; Flygare, W. H. *Rev. Sci. Instrum.* **1981**, *52*, 33. (b) Dreizler, H. *Ber. Bunsen-Ges. Phys. Chem.* **1995**, *99*, 1451.
(23) Phillips, J. A. Ph.D. Thesis, University of Minnesota, 1996.
(24) Legon, A. C. *Chem. Commun.* **1996**, 109.
(25) Gillies, C. W.; Gillies, J. Z.; Suenram, R. D.; Lovas, F. J.; Kraka, E.; Cremer, D. *J. Am. Chem. Soc.* **1991**, *113*, 2412.
(26) Gutowsky, H. S.; Chen, J.; Hajduk, P. J.; Keen, J. D.; Emilsson, T. *J. Am. Chem. Soc.* **1989**, *111*, 1901.
(27) Emilsson, T.; Klots, T. D.; Ruoff, R. S.; Gutowsky, H. S. *J. Chem. Phys.* **1990**, *93*, 6971.
(28) Bowen, K. H.; Leopold, K. R.; Chance, K. V.; Klemperer, W. *J. Chem. Phys.* **1980**, *73*, 137.
(29) Coudert, L. H.; Lovas, F. J.; Suenram, R. D.; Hougen, J. T. *J. Chem. Phys.* **1987**, *87*, 6290.
(30) Wollrab, J. E.; Laurie, V. W. *J. Chem. Phys.* **1969**, *51*, 1580.
(31) (a) Kaldor, A.; Maki, A. G. *J. Mol. Struct.* **1973**, *15*, 123. (b) Meyer, V.; Sutter, D. H.; Dreizler, H. *Z. Naturforsch., A* **1991**, *46*, 710.
(32) (a) *Organic Synthesis*, 2nd ed.; Wiley: New York, 1964; Collect. Vol. 1. (b) Clippard, P. H. Ph.D. Thesis, University of Michigan, 1969.
(33) Gordy, W.; Cook. R. L. *Microwave Molecular Spectra*; Wiley: New York, 1984.

Table 1. Observed Transitions of $(CH_3)_3{}^{14}N-{}^{32}SO_3$[a]

J''	F''	K	J'	F'	frequency[b] (MHz)	obsd − calcd (MHz)
0	1	0	1	1	3 266.565	−0.002
0	1	0	1	2	3 267.024	−0.002
0	1	0	1	0	3 267.715	0.001
1	2	0	2	2	6 533.431	−0.004
1	0	0	2	1	6 533.509	−0.002
1	1	1	2	2	6533.509	−0.002
1	2	1	2	2	6 533.738	−0.002
1	1	0	2	2	6 533.892	−0.002
1	1	1	2	1	6 533.892	−0.002
1	2	0	2	3	6 533.925	−0.002
1	2	1	2	3	6 533.987	0.000
1	2	1	2	1	6 534.121	−0.002
1	2	0	2	1	6 534.200	−0.000
1	0	1	2	1	6 534.471	0.003
1	1	0	2	1	6 534.659	−0.000
2	3	0	3	3	9 800.336	−0.002
2	2	2	3	2	9 800.455	0.008
2	2	2	3	3	9 800.455	0.008
2	3	1	3	3	9 800.486	−0.002
2	2	1	3	3	9 800.731	−0.003
2	1	0	3	2	9 800.760	0.007
2	2	0	3	3	9 800.835	0.005
2	3	0	3	4	9 800.847	−0.001
2	3	1	3	4	9 800.869	−0.002
2	1	1	3	2	9 800.869	0.001
2	3	2	3	4	9 800.942	0.003
2	3	2	3	3	9 800.942	0.003
2	3	2	3	2	9 800.942	0.003
2	1	2	3	2	9 801.213	0.000
2	2	1	3	2	9 801.249	−0.002
2	2	0	3	2	9 801.517	−0.002
3	4	0	4	4	13 067.242	−0.001
3	3	3	4	4	13 067.409	0.000
3	2	0	4	3	13 067.717	−0.003
3	3	1	4	4	13 067.717	0.002
3	3	0	4	4	13 067.756	0.003
3	2	1	4	3	13 067.756	0.000
3	4	0	4	5	13 067.769	0.004
3	4	1	4	5	13 067.774	−0.002
3	4	2	4	5	13 067.813	0.004
3	4	3	4	3	13 067.813	−0.004
3	2	2	4	3	13 067.861	−0.002
3	3	2	4	3	13 067.861	−0.002
3	4	3	4	5	13 067.861	−0.003
3	4	2	4	3	13 067.861	−0.002
3	2	3	4	3	13 068.042	0.002
3	4	3	4	4	13 068.042	−0.004
3	3	1	4	3	13 068.272	−0.001
3	3	0	4	3	13 068.409	0.000

[a] $\mathbf{F = I(N) + J}$. [b] The estimated uncertainty in measured frequencies is ±3 kHz.

observed frequencies was performed with B, D_J, and eQq constrained to their values determined at zero electric field. This fit yielded the ratio of the molecular dipole moment to the effective interplate spacing from which the molecular dipole moment was calculated using the $Ar-SO_3$ calibration results. The dipole moment of the complex was determined to be 7.1110(69) D.

Structure Analysis. The observation of a symmetric top spectrum as well as the results of the isotopic substitution experiments confirm the expected geometry in which the nitrogen lone pair is directed toward the sulfur along the C_3 axis of the SO_3. Preliminary analysis of the observed rotational constants indicated an N−S distance of approximately 1.90 Å, a value which is slightly larger than the 1.844(2) Å distance observed in solid TMA-SO_3[18] but significantly shorter than the 2.9 Å distance expected for a nitrogen−sulfur van der Waals

Table 2. Observed Transitions of $(CH_3)_3{}^{14}N-{}^{34}SO_3$[a]

J''	F''	K	J'	F'	frequency[b] (MHz)	obsd − calcd (MHz)
1	2	0	2	2	6500.595	0.000
1	0	0	2	1	6500.671	−0.001
1	1	1	2	2	6500.671	−0.001
1	2	1	2	2	6500.902	0.000
1	1	0	2	2	6501.054	−0.002
1	1	1	2	1	6501.054	−0.002
2	3	0	3	3	9751.076	−0.001
1	2	0	2	3	6501.086	−0.003
1	2	1	2	3	6501.153	0.004
1	0	1	2	1	6501.634	0.002
1	1	0	2	1	6501.823	−0.001
2	2	2	3	2	9751.191	0.004
2	2	2	3	3	9751.191	0.004
2	3	1	3	3	9751.220	−0.008
2	2	1	3	3	9751.472	−0.003
2	1	0	3	2	9751.499	0.005
2	2	0	3	3	9751.574	0.003
2	3	0	3	4	9751.589	0.000
2	3	1	3	4	9751.610	−0.002
2	1	1	3	2	9751.610	0.001
2	3	2	3	4	9751.682	0.002
2	3	2	3	3	9751.682	0.002
2	3	2	3	2	9751.682	0.002
2	1	2	3	2	9751.958	0.004
2	2	1	3	2	9751.982	−0.011
2	2	0	3	2	9752.262	0.001

[a] $\mathbf{F = I(N) + J}$. [b] The estimated uncertainty in measured frequencies is ±3 kHz.

Table 3. Observed Transitions of $(CH_3)_3{}^{14}N-{}^{33}SO_3$[a]

J''	F_1''	F''	K	J'	F_1'	F'	frequency[b] (MHz)	obsd − calcd (MHz)
2	3.5	4.5	0	3	3.5	4.5	9771.213	−0.001
2	1.5	2.5	0	3	2.5	3.5	9775.018	0.006
2	1.5	1.5	1	3	2.5	2.5	9775.054	0.000
2	2.5	2.5	1	3	3.5	3.5	9775.105	0.002
2	0.5	0.5	0	3	1.5	0.5	9775.214	−0.002
2	2.5	3.5	1	3	3.5	4.5	9775.260	−0.007
2	2.5	2.5	0	3	3.5	3.5	9776.047	−0.001
2	3.5	3.5	0	3	4.5	4.5	9776.130	−0.001
2	3.5	4.5	1	3	4.5	4.5	9776.154	0.004
2	3.5	2.5	0	3	4.5	3.5	9776.154	0.009
2	3.5	4.5	0	3	4.5	5.5	9776.180	0.002
2	0.5	0.5	1	3	1.5	1.5	9776.220	−0.014
2	3.5	3.5	1	3	4.5	4.5	9776.355	0.000
2	0.5	1.5	1	3	1.5	2.5	9776.474	0.010
2	3.5	4.5	1	3	4.5	5.5	9776.496	0.002
2	3.5	2.5	1	3	4.5	3.5	9776.517	0.011
2	2.5	2.5	1	3	2.5	2.5	9776.891	−0.004
2	2.5	3.5	1	3	2.5	3.5	9776.976	−0.004
2	2.5	1.5	1	3	2.5	1.5	9777.008	−0.011

[a] $\mathbf{F_1 = I(S) + J}$; $\mathbf{F = F_1 + I(N)}$. [b] The estimated uncertainty in measured frequencies is ±3 kHz.

interaction.[5a] Thus, the structure analysis was performed using standard methods appropriate for valence-bonded systems.[33]

With only six rotational constants to be analyzed, a full determination of all atomic coordinates in the complex is not possible. However, several reasonable constraints can be applied which allow the chemically interesting structural features of the system to be obtained. In particular, we note that the TMA unit does not change significantly upon formation of the solid adduct. For example, the N−C bond length and CNC angle reported in crystalline TMA−SO_3[18] differ from those in gas-phase TMA[30] by only 0.045 Å and 1.8°, respectively. Similarly, we find an expansion of the S−O bond length of only 0.0148 Å between gaseous SO_3[31] and the crystalline complex. These changes are small and suggest that neither the structure of the TMA unit

Table 4. Observed Transitions of ^{15}N Containing Derivatives of $(CH_3)_3N-SO_3$[a,b]

isotopomer	J''	F''	K	J'	F'	frequency (MHz)	(O−C) (MHz)
$(CH_3)_3{}^{15}N-{}^{32}SO_3$	0		0	1		3 256.199	0.000
	1		0	2		6 512.390	−0.003
	2		0	3		9 768.577	−0.002
	3		0	4		13 024.753	0.003
$(CH_3)_3{}^{15}N-{}^{34}SO_3$	0		0	1		3 239.617	−0.002
	1		0	2		6 479.234	0.000
	2		0	3		9 718.841	0.000
	3		0	4		12 958.437	0.000
$(CH_3)_3{}^{15}N-{}^{33}SO_3$							
	1	0.5	0	2	0.5	6 495.626	−0.004
	1	2.5	0	2	3.5	6 496.053	0.001
	1	1.5	0	2	2.5	6 496.053	0.001
	1	2.5	1	2	3.5	6 496.823	−0.001
	2	1.5	0	3	2.5	9 742.452	0.001
	2	0.5	0	3	1.5	9 742.452	0.001
	2	1.5	2	3	2.5	9 743.438	0.003
	2	1.5	2	3	1.5	9 743.438	0.003
	2	3.5	0	3	4.5	9 743.670	0.001
	2	3.5	0	3	3.5	9 743.747	−0.004
	2	3.5	1	3	4.5	9 743.965	0.003
	2	3.5	2	3	4.5	9 744.840	0.000
	2	3.5	2	3	3.5	9 744.840	0.000
	2	2.5	0	3	2.5	9 745.963	−0.001
	2	1.5	0	3	1.5	9 747.365	−0.004

[a] The estimated uncertainty in measured frequencies is ±3 kHz. [b] $\mathbf{F} = \mathbf{I(S)} + \mathbf{J}$.

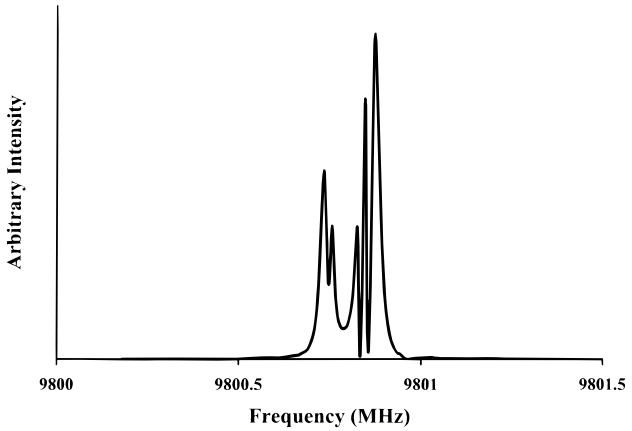

Figure 1. The $J = 3 \leftarrow 2$ transition of $(CH_3)_3{}^{14}N-{}^{32}SO_3$ showing several hyperfine components due to the ^{14}N nucleus. The total signal collection time for this spectrum was 16 s.

Table 5. Spectroscopic Constants for $(CH_3)_3N-SO_3$[a]

isotopomer	B (MHz)	D_J (MHz)	$eQq(^{14}N)$ (MHz)	$eQq(^{33}S)$ (MHz)
$(CH_3)_3{}^{14}N-{}^{32}SO_3$	1633.4749(1)	0.177(12)	−1.5303(34)	
$(CH_3)_3{}^{15}N-{}^{32}SO_3$	1628.0999(5)	0.188(13)		
$(CH_3)_3{}^{14}N-{}^{34}SO_3$	1625.2657(2)	0.215(63)	−1.5352(44)	
$(CH_3)_3{}^{15}N-{}^{34}SO_3$	1619.8097(5)	0.1579(77)		
$(CH_3)_3{}^{15}N-{}^{33}SO_3$	1629.3243(3)	0.18[b]	−1.513(15)	−19.673(25)
$(CH_3)_3{}^{15}N-{}^{33}SO_3$	1623.9087(3)	0.161(35)		−19.672(14

[a] Uncertainties are 1 standard error in the least-squares fits. [b] Held fixed in fit.

nor the S−O bond length need be redetermined from the present data. The dimensionality of the problem can thus be reduced to an acceptable level by constraining the structure of the TMA and the S−O bond distance while still retaining the N−S bond length and NSO bond angle as determinable parameters.

The nitrogen−sulfur bond length, R, and the NOS bond angle, α, were obtained from least-squares fits to the observed rotational constants with the remaining bond lengths and bond

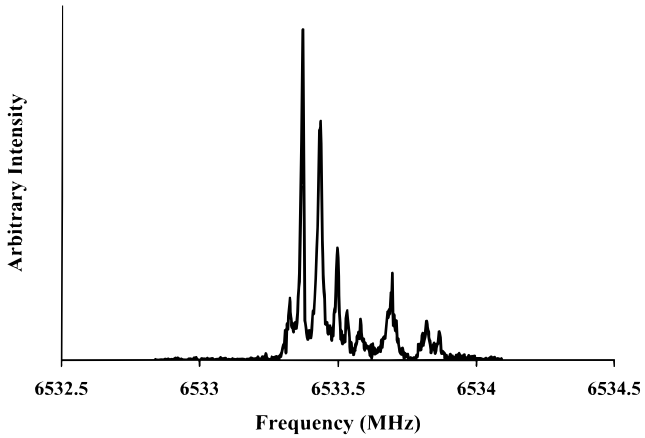

Figure 2. A portion of the $J = 2 \leftarrow 1$ transition of $(CH_3)_3{}^{14}N-{}^{32}SO_3$ taken at an applied electric field of 18.59 V/cm. The signal collection time for this spectrum was 25 s.

Table 6. Comparison of $(CH_3)_3N-SO_3$ and H_3N-SO_3

	$(CH_3)_3N-SO_3$		H_3N-SO_3	
parameter	gas[a]	solid[b]	gas[c]	solid
R(NS) (Å)	1.912(20)	1.844(2)	1.957(23)	1.7714(3)[d]
α(NSO) (deg)	100.1(2)	101.8(1)	97.6(4)	102.5(8)[d]
no. of e	0.58		0.36	
μ (D)	7.1110(69)		6.204(11)	9.6(6)[e]
μ_{find}[f] (D)	6.50(1)		4.73(1)	

[a] This work. [b] Reference 18. [c] Reference 5. [d] Reference 14. [e] Reference 35. [f] $\mu_{ind} \equiv \mu(\text{complex}) - \mu(NR_3) - \mu(SO_3) = \mu(\text{complex}) - \mu(NR_3)$.

angles constrained as described above. Since the choice of crystallographic vs free-monomer values for the constrained parameters introduces the primary source of uncertainty into R and α, two fits were performed. The first employed the TMA structure and SO bond distance observed in solid $TMA-SO_3$, and resulted in values of R and α of 1.892 Å and 99.86°, respectively. The second used the gas-phase monomer values for the constrained parameters and resulted in R and α values of 1.932 Å and 100.32°, respectively.

It is clear that regardless of the choice of the S−O bond length or TMA structural parameters, the fitted N−S distance and NSO angle lie between those of a hypothetical van der Waals complex and those observed in the crystal. Correspondingly, we expect that the remaining structural parameters of the complex will lie between those of the free monomers and those observed in the solid. Thus, the results of the two fits provide a reasonable window within which the true structural parameters of the gas-phase species are likely to lie.[34] The preferred values of R and α, therefore, are taken as the average of two fits, with the uncertainties chosen to encompass both determinations. These results are given in Table 6, and the structure of the complex is shown in Figure 3. Note that the rotational constants do not depend on the torsional angle between the TMA and SO_3 units,

(34) It might be argued that, in view of the similarity of the N−S bond length to that in the solid, the fit employing the crystal-phase parameters gives the more reasonable numbers. However, it is likely that the changes in monomer structure which occur as the dative bond forms take place at short distances where the orbital overlap is most substantial. Thus, even at the gas-phase structure of the complex, the changes in the TMA structure and SO bond length may not yet be those observed in the crystal. Moreover, it is likely that these changes result, to some degree, from forces acting in the crystal, in which case, again, the crystal-phase parameters are not necessarily more valid than the free monomer values.

(35) Coppens, P.; Guru Row, T. N.; Leung, P.; Stevens, E. D.; Becker, P. J.; Yang, Y. W. *Acta Crystallogr.* **1979**, *A35*, 63.

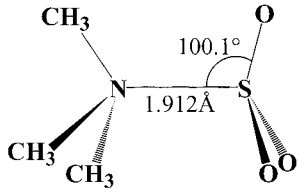

Figure 3. Structure of trimethylamine−sulfur trioxide in the gas phase. The torsional angle between the $(CH_3)_3N$ and SO_3 moieties is not determined in this work.

and thus the relative configuration (staggered vs eclipsed) cannot be determined in this study.

As an independent check of the above results, a Kraitchman analysis was performed[33] to determine the N−S bond length. This method has the advantage of giving the N−S distance directly from isotopic substitution of the nitrogen and sulfur without the need for supplementary approximations about the position of other atoms in the complex. Its disadvantage is that with the present data set, the NSO angle cannot be determined. Nevertheless, with this approach, an average value of 1.915 Å is obtained for the N−S bond distance, which is in almost exact agreement with the 1.912 Å value reported in Table 6.

Discussion

Molecular Structure. Table 6 compares the gas-phase structural parameters determined above with those previously published for the adduct in the solid state. Also included are the corresponding values for H_3N-SO_3. It is apparent that the gas-phase bond length of the TMA complex exceeds that in the solid by 0.068(22) Å, which represents a modest, but nevertheless significant contraction upon crystallization. The NSO angle displays a correspondingly small increase between the gas phase and solid state (1.7° ± 0.3°). These changes are smaller than those observed for H_3N-SO_3, but are in the same direction and indicate that the dative bond is driven toward completion by the crystallization process.

The gas-phase bond length in $TMA-SO_3$ is very similar to that in gaseous H_3N-SO_3. That the value appears slightly *shorter* and that the NSO bond angle 2.5° *larger* is consistent with the increased basicity of TMA relative to ammonia. Interestingly, however, in the solid state, the ammonia complex has a shorter bond length and larger bond angle, and it is this reversal which largely accounts for the smaller gas-to-solid structure changes observed in the TMA adduct. Moreover, it is perhaps significant to note that the sum of ordinary covalent bond radii for nitrogen and sulfur is 1.74 Å,[36] which is very close to the N−S distance observed in crystalline H_3N-SO_3. On this basis it appears that the bond in H_3N-SO_3 is driven virtually to completion in the solid, while that in the TMA complex is not. This relationship between the crystal structures and the degree of dative bond formation in these systems is discussed in the final section of this paper.

Electronic Structure. Two aspects of the electronic structure of the complex can be elucidated from the data obtained in this work. The dipole moment is determined directly from the spectroscopic measurements, as described above. Moreover, a measure of the degree of electron transfer upon dative bond formation is accessible via interpretation of the ^{14}N nuclear quadrupole coupling constants given in Table 5. These two features of the system are discussed in this section.

The dipole moment of 7.1110(69) D determined for $TMA-SO_3$ in the gas phase is indicative of significant charge rearrangement upon complexation. Indeed, for free TMA and SO_3, the dipole moments are only 0.612(3) D[37] and 0 D,[36] respectively. Thus, the formation of the adduct generates an induced moment of 6.50 D. This value is given in Table 6, as is the corresponding value for the NH_3 complex. It is significant to note that although the dipole moment of ammonia (1.47149(15) D[38]) is substantially larger than that of TMA, the induced moment in $TMA-SO_3$ exceeds that in H_3N-SO_3 by more than 1.7 D. Thus, it is clear that the induced moment contains significant contributions from sources other than electrostatic polarization. This is reasonable in light of the increased basicity of TMA relative to that of NH_3 and its correspondingly greater tendency for dative bond formation. The shorter gas-phase bond length and larger NSO angle in the TMA complex further reflect this trend.

The ^{14}N nuclear quadrupole coupling constants in Table 5 are also consistent with this picture. These constants depend on the electric field gradient at the coupling nucleus and may be interpreted in a simple manner by the well-known method of Townes and Dailey.[33,39] In essence, for atoms in the first row of the periodic table, the electric field gradient at the nucleus is dominated by the population of valence p electrons. Thus, changes in the coupling constant upon complexation reflect the loss of p electron density to the acceptor.

To implement the method, the one-electron wave function for the dative bond between the TMA and SO_3 is written as $\psi = \alpha\phi_N + \beta\phi_S$, where ϕ_N is the approximately sp^3-hybridized nitrogen lone-pair orbital and ϕ_S is the acceptor orbital on the SO_3. We are careful to speak of electron transfer "to SO_3" (rather than just sulfur) because of the delocalization of electron density onto the oxygens. The squares of the coefficients, α and β, represent the electron population on the nitrogen and the SO_3, respectively. Using this wave function, the reduction in nitrogen quadrupole coupling constant upon formation of the dative bond is given by[5a,40,41]

$$[(eQq)_{complex} - (eQq)_{TMA}] = -6a_s^2(eQq_{210})(1 - \alpha^2) \quad (4)$$

where $(eQq)_{complex}$ is the ^{14}N quadrupole coupling constant in the complex and $(eQq)_{TMA}$ is that of free TMA. a_s^2 represents the amount of s character in the N−C σ bonds of TMA, and (eQq_{210}) is the quadrupole coupling constant for a single $2p_z$ electron in atomic nitrogen. The value of a_s^2 can be obtained from the estimated CNC bond angle in the complex, γ, according to[41]

$$a_s^2 = (\cos\gamma)/(\cos\gamma - 1) \quad (5)$$

Using $\gamma = 110.0°$ (intermediate between that of free TMA and solid $TMA-SO_3$), $eQq_{210} = -9.0$ MHz,[41] and $eQq_{TMA} = -5.5024(25)$ MHz,[42] a value of $1 - \alpha^2 = 0.289$ is obtained. For 2 e in the dative bond, this corresponds to a total electron transfer of 0.58 e from the nitrogen to the SO_3. This result and the corresponding value obtained previously for H_3N-SO_3[5a]

(36) Cotton, F. A.; Wilkinson, G. *Advanced Inorganic Chemistry*, 3rd ed.; Interscience: New York, 1972.
(37) Lide, D. R., Jr.; Mann, D. E. *J. Chem. Phys.* **1958**, *28*, 572.
(38) Marshall, M. D.; Muenter, J. S. *J. Mol. Spectrosc.* **1981**, *85*, 322.
(39) Townes, C. H.; Dailey, B. P. *J. Chem. Phys.* **1949**, *17*, 782.
(40) Oh, J. J.; LaBarge, M. S.; Matos, J.; Kampf, J. W.; Hillig, K. W., II; Kuczkowski, R. L. *J. Am. Chem. Soc.* **1991**, *113*, 4732.
(41) Lucken, E. A. C. *Nuclear Quadrupole Coupling Constants*; Academic Press: New York, 1969.
(42) Rego, C. A.; Batten, R. C.; Legon, A. C. *J. Chem. Phys.* **1988**, *89*, 696.

Table 7. Selected Solid-Phase Structural Parameters for the $H_{3-n}(CH_3)_nN-SO_3$ Systems

	$(CH_3)_3N-SO_3$[a]	$H(CH_3)_2N-SO_3$[b]	$H_2CH_3N-SO_3$[c]	H_3N-SO_3[d]
N−S (Å)	1.844(2)	1.790(6)	1.779(8)	1.7714(3)
S−O (Å)[e]	1.405(2)	1.430(5)	1.425(8)	1.442(3)
N−S−O (deg)[e]	101.8(1)	102.1(3)	102.4(7)	102.5(8)

[a] Reference 18. [b] Reference 45. [c] Reference 46. [d] Reference 14. [e] Average over crystallographically distinct values.

are also included in Table 6. Note that while it would be desirable, in principle, to perform a complementary analysis of the ^{33}S quadrupole coupling constants in Table 5, such a possibility is precluded by the absence of a suitably simple orbital description of the SO_3.

The result of the above calculations indicates that in TMA−SO_3, the degree of electron transfer is significantly larger than that in H_3N-SO_3. This is a pleasing result, as it is consistent with the increased basicity of TMA relative to ammonia and therefore with the trends in bond length, bond angle, and induced dipole moment noted above. It is also satisfying in light of previous work with the weaker Lewis acid, SO_2. In TMA−SO_2,[40] where the N−S bond length is correspondingly longer than that in TMA−SO_3 (2.26 ± 0.03 Å vs 1.91 ± 0.02 Å), quadrupole coupling data indicate only about 0.24 e transferred upon complexation.

While these comparisons are all very sensible, it should be emphasized that the form of the dative bond wave function used in the calculations, as well as the method of Townes and Daily itself, is extremely crude. Thus, the resulting values of the electron transfer are approximate. Indeed, it is noteworthy that, in H_3N-SO_3, a quantum topological analysis gives a "charge transfer" of 0.28 e,[17] which appears to be, at least superficially, in reasonable agreement with the 0.36 e value obtained experimentally. However, the analysis also indicates[17] that the largest changes in charge upon complex formation take place on the hydrogens and the oxygens, a feature which cannot be described by the simplistic dative bond wave function used above. Despite these comments, however, we note that the Townes and Dailey analysis has long provided a wealth of chemical information from quadrupole coupling constants[33,41] and the results obtained here, taken with an appropriate level of caution, present a simple and consistent picture of the changes which occur upon methylation of H_3N-SO_3.

Finally, it is of interest to return to the question of the origin of the large induced moments in both H_3N-SO_3 and TMA−SO_3. In our previous work on the ammonia complex,[5b] we showed that a very simple model could be used to recover a large portion of the experimentally determined moment. In this model, three terms contribute to the observed moment: (i) the dipole moment of the amine moiety, taken to be that of the free amine, (ii) the dipole moment of the pyramidally distorted SO_3 moiety, calculated from an SO bond moment of 3 D,[43] and (iii) a charge-transfer component obtained from the product of the NS bond length and the number of electrons transferred (the latter determined from the Townes and Dailey analysis). The value obtained for H_3N-SO_3 was 6.1 D, which agrees with the experimental determination to within 2%.

As we have noted previously,[5b] the above calculation omits contributions due to polarization. Furthermore, the use of the N−S bond length is not necessarily correct. Thus, the remarkable agreement with experiment may be fortuitous, and it is therefore useful to have another system with which to test the model. In the case of TMA−SO_3, the dipole moment of the amine is 0.612 D,[37] that of the pyramidally distorted SO_3 is 1.58 D, and the charge-transfer component is 5.33 D. The sum of these values is 7.52 D, which is only 6% higher than the experimentally determined dipole moment. The agreement is, once again, astounding and suggests that (as in the case of H_3N-SO_3) a large portion of the induced moment arises from charge transfer between the donor and acceptor. It is interesting to observe (Table 6) that the large changes in both electron transfer and dipole moment accompany a relatively modest contraction of the N−S bond between H_3N-SO_3 and $(CH_3)_3N-SO_3$. Such an observation suggests that much of the charge redistribution which occurs upon complex formation does so at very short distances.

Comparison of Crystalline TMA−SO_3 and H_3N-SO_3. As noted above, the acid−base interaction in TMA−SO_3 is expected to be stronger than that in H_3N-SO_3 because of the greater basicity of TMA. However, while the N−S bond distance and NSO bond angle in the gas-phase complexes are consistent with this notion, the solid-state structural data are not. Hargittai and Hargittai have shown that small gas-to-solid structure differences can be meaningfully interpreted in a wide variety of systems,[44] and it is of interest to see whether the amine−SO_3 data presented here can be similarly understood.

Table 7 compares structural parameters for the series of sulfamic acid complexes with the general formula $H_{3-n}(CH_3)_nN-SO_3$. Although in some cases the uncertainties are large enough to preclude a meaningful comparison between adjacent members of the series, two overall trends emerge. First, as the number of methyl groups increases, the N−S bond elongates. Second, with increasing methylation, the S−O bond length decreases. This latter effect is difficult to discern for the mono- and dimethylated species given the uncertainties, but is apparent for the H_3N and $(CH_3)_3N$ adducts. These trends have been noted previously[45,46] and are consistent with a weakening of the dative interaction upon methylation. The NSO bond angles, unfortunately, are neither consistent nor inconsistent with this picture, given the experimental uncertainties and range of crystallographically distinct angles. Curiously, the S−O bond length in TMA−SO_3 appears anomalous in that it is *shorter* than the 1.4198(2) Å value observed in free SO_3.[31] The reason for this is not clear.[47]

We have previously established[1−11] that dative bonds whose formation is incomplete in the gas phase are strongly susceptible to the influence of a crystalline environment. Moreover, there is evidence, from both the calculation of lattice sums[40] and application of SCRF methods,[17,48,49] that this effect may be

(43) Huheey, J. E. *Inorganic Chemistry*, 3rd ed.; Harper and Row: New York, 1983.
(44) (a) Hargittai, I.; Hargittai, M. In *Molecular Structure and Energetics*; Liebman, J. F., Greenberg, A., Eds.; VCH Publishers: Deerfield Beach, FL, 1987; Vol. 2, p 1. (b) Hargittai, M.; Hargittai, I. *Phys. Chem. Miner.* **1987**, *14*, 413 and references therein.
(45) Morris, A. J.; Kennard, C. H. L.; Hall, J. R.; Smith, G. *Inorg. Chim. Acta* **1982**, *62*, 247.
(46) Morris, A. J.; Kennard, C. H. L.; Hall, J. R. *Acta Crystallogr.* **1983**, *C39*, 1236.
(47) To check the possibility of a typographical error in the published SO bond length in solid TMA−SO_3, we regenerated the structure from available crystal data and found agreement with the value cited in ref 18.
(48) Jiao, H.; Schleyer, P.v.R. *J. Am. Chem. Soc.* **1994**, *116*, 7429.
(49) Buhl, M.; Steinke, T.; Schleyer, P.v.R.; Boese, R. *Angew. Chem., Int. Ed. Engl.* **1991**, *30*, 1160.

understood (at least to a first approximation) in terms of the dipole moment functions for these systems. In particular, since the dipole moments increase as the dative bond forms, the bonding advances upon crystallization to lower the total intermolecular interaction energy in the solid. The gas-phase and solid-state dipole moments given in Table 6 for H_3N-SO_3 illustrate the magnitude of the change in dipole moment which can occur in these types of systems.

To see whether the observed anomaly in the crystal structure of the amine$-SO_3$ complexes could be understood in terms of this mechanism, packing plots were generated for H_3N-SO_3[14] and TMA$-SO_3$[18] from published crystallographic data. These plots, together with similar diagrams for $CH_3H_2N-SO_3$[46] and $(CH_3)_2HN-SO_3$, are available as Supporting Information. As expected, the bulkiness of the three methyl groups in TMA$-SO_3$ has a large effect on packing in the molecular solid. Individual monomer units line up unidirectionally in one-dimensional chains, with the SO_3 end of one molecule directed toward the TMA end of a second molecule. The oxygen-to-hydrogen distance is 3.0 Å. Neighboring chains are staggered relative to one another, with the distance between an N$-$S bond in one chain and the closest methyl carbon on a neighboring chain being 4.8 Å. Successive layers of TMA$-SO_3$ chains fit into the grooves between the chains below, ensuring tight packing.

In contrast, H_3N-SO_3 crystallizes in a complex 3-dimensional network exhibiting extensive intermolecular hydrogen bonding, with H$\cdots$O distances ranging from 1.918 to 2.404 Å. Throughout this intricate network are series of antiparallel H_3N-SO_3 pairs, wherein each nearest neighbor is related to its partner by a 180° rotation about one of the two equivalent principal axes of the monomer. The distance between the center of the N$-$S bond in one monomer to that in its nearest anti-aligned neighbor is 3.9 Å, almost a full angstrom shorter that the equivalent distance in TMA$-SO_3$(s).

In view of these observations, it may be possible to rationalize the differences between crystalline H_3N-SO_3 and TMA$-SO_3$. Due to the bulkiness of the methyl groups, the optimum spatial arrangement of molecules in TMA$-SO_3$ produces fewer and more distant intermolecular contacts than in the case of H_3N-SO_3. Thus, interactions between adjacent dipoles and consequently the capacity of near-neighbor interactions to drive the formation of individual N$-$S bonds are reduced. Moreover, the differences are likely to be compounded by the propensity for hydrogen bonding in the ammonia complex, which gives rise to especially strong intermolecular interactions. The overall picture, then, is that, in TMA$-SO_3$, the unidirectionality of the interactions, the larger intermolecular distances, and the lack of hydrogen bonding diminish the ability of dipolar interactions in the solid to stabilize the charge separation associated with the advancement of the dative bond. Thus, while the N$-$S bond in the ammonia complex can be driven essentially to completion, that in the TMA adduct is not. Moreover, we may infer that, in $CH_3H_2N-SO_3$ and $(CH_3)_2HN-SO_3$, both the bulkiness of the amine and the opportunities for hydrogen bonding are between those of the H_3N-SO_3 and $(CH_3)_3N-SO_3$. Hence, it is perhaps not too surprising that the physical properties listed in Table 7 progress as they do across the series. Close scrutiny of the stereoscopic projections for these crystal systems indicates that they are consistent with such an idea.

Conclusions

Microwave spectroscopy has been used to investigate the molecular and electronic structures of $(CH_3)_3N-SO_3$ in the gas phase. The N$-$S bond length is 1.912(20) Å, and the NSO angle is 100.1(2)°, indicating a dative bond which is nearly, but not entirely, formed. Analysis of the ^{14}N nuclear hyperfine structure indicates that about 0.6 e is transferred from the trimethylamine to the SO_3 upon formation of the adduct, and Stark effect measurements reveal a gas-phase dipole moment of 7.1110(69) D. These results are consistent with significant charge redistribution upon complex formation. The degree of charge transfer between the donor and acceptor is nearly twice that observed in the related complex H_3N-SO_3, and the induced dipole moment is 1.8 D larger. These changes are particularly interesting in light of the more modest difference in N$-$S bond lengths between the two compounds. The trends in bond length, electron transfer, and induced moment, however, are consistent with the greater basicity of $(CH_3)_3N$ relative to that of ammonia.

The observed N$-$S bond length in the gas phase is longer than that previously reported for the crystalline adduct, and the NSO angle is smaller. These differences indicate that the crystallization of the complex drives the dative bond toward completion. Interestingly, however, while the N$-$S bond length is shorter than that of the NH_3 complex in the gas phase, it is longer in the crystal. This anomaly can be rationalized in the context of previous work on medium effects in donor$-$acceptor systems, and by close examination of packing plots generated from published crystallographic data. In essence, the larger intermolecular distances resulting from the methyl groups, as well as the lack of hydrogen-bonding interactions present in the ammonia adduct, render the crystallization of TMA$-SO_3$ less effective at driving the charge separation associated with the formation of the dative bond.

Acknowledgment. This work was supported by the National Science Foundation and the donors of the Petroleum Research Fund, administered by the American Chemical Society. A.T. was supported by a Lando-NSF-REU Summer Undergraduate Research Fellowship at the University of Minnesota. We, especially D.L.F., acknowledge Dr. M. Pink for assistance in attaining and analyzing the crystallographic packing plots.

Supporting Information Available: Table giving Stark shifted hyperfine frequencies at varying electric fields and figures showing stereoscopic projections for H_3N-SO_3, $CH_3H_2N-SO_3$, $(CH_3)_2HN-SO_3$, and $(CH_3)_3N-SO_3$. This material is available free of charge via the Internet at http://pubs.acs.org.

IC990925J